Advances in Water Resources xxx (2012) xxx–xxx

Contents lists available at SciVerse ScienceDirect

Advances in Water Resources

journal homepage: www.elsevier.com/locate/advwatres

Estimation of surface energy fluxes using surface renewal and flux variance techniques over an advective irrigated agricultural site ☆

Andrew N. French [a,*], Joseph G. Alfieri [b], William P. Kustas [b], John H. Prueger [c], Lawrence E. Hipps [d], José L. Chávez [e], Steven R. Evett [f], Terry A. Howell [f], Prasanna H. Gowda [f], Douglas J. Hunsaker [a], Kelly R. Thorp [a]

[a] U.S. ALARC, 21881 North Cardon Lane, Maricopa, AZ 85138, United States
[b] USDA-ARS Hydrology and Remote Sensing Laboratory, Beltsville, MD 20705, United States
[c] USDA-ARS National Laboratory for Agriculture and Environment, Ames, IA 5001, United States
[d] Utah State University, Dept. of Plants, Soils, and Biometeorology, Logan, UT 84322, United States
[e] Colorado State University, Dept. of Civil and Environmental Engineering, Fort Collins, CO 80523, United States
[f] USDA-ARS Conservation and Production Laboratory, Bushland, TX 79012, United States

ARTICLE INFO

Article history:
Available online xxxx

Keywords:
Surface renewal
Flux variance
Advection
Cotton heat flux
Irrigated cotton
BEAREX08

ABSTRACT

Estimation of surface energy fluxes over irrigated agriculture is needed to monitor crop water use. Measurements are commonly done using well-established techniques such as eddy covariance (EC) and weighing lysimetry, but implementing these to collect spatially distributed observations is complex and costly. Two techniques that could simplify flux observations are the surface renewal (SR) and flux variance (FV) approaches. These methods infer sensible heat fluxes from high frequency observations of near surface air temperatures using low cost thermocouples. In combination with net radiation and soil heat flux observations, surface renewal and flux variance observations produce latent heat fluxes as a residual of the surface energy balance. The viability of these techniques was tested in a strongly advective irrigated agricultural setting as part of the Bushland Evapotranspiration and Agricultural Remote Sensing Experiment in 2008 (BEAREX08). Using 20 Hz air temperature data collected between 12 June and 13 August from two cotton field sites and one senescent/dormant grass site, sensible heat flux estimates were computed. Surface flux conditions ranged widely and include episodes of latent heat fluxes exceeding net radiation. Overall, flux estimates from SR and FV were similar to simultaneously obtained eddy covariance observations on most days. During strong advection neither approach closely agreed with EC data, although the surface renewal technique more reliably estimated the correct sign of sensible heat fluxes. Both techniques were found to offer flux estimates comparable to EC data, though with different advantages. SR is self-contained, requiring no additional instrumentation beyond air temperature equipment. SR correctly diagnosed the sign of sensible heat fluxes and produced better estimates at early morning and late afternoon times than FV, although these were achieved after lag time selection using EC data for calibration. FV, by contrast, required wind speed observations, as well as thermal infrared data to resolve heat flux directions. However, using nominal parameters and no local calibration, FV produced mid-day estimates equal to or better than SR. These outcomes indicate that flux data with accuracies approaching EC capabilities is feasible with the potential for reduced deployment complexity and cost.

Published by Elsevier Ltd.

1. Introduction

Accurate, spatially distributed estimation of the surface energy balance is crucial for monitoring crop water use and evaluating daily to seasonal water budgets. In the past few decades, robust instruments have become routinely available to precisely measure the four main energy flux components: net radiation (R_n), soil heat (G), sensible heat (H), and latent heat (LE). The first two components, measured with net radiometers and soil heat flux plates, do pose challenges with representativity because of their small footprint, but generally they can be estimated in relatively simple and affordable ways. The latter two components, on the other hand, require complex and delicate systems that are expensive to distribute throughout a study area on a routine basis. Distributed systems are required for experiments within highly heterogeneous systems such as irrigated agriculture. These systems include eddy

☆ USDA is an equal opportunity provider and employer.

* Corresponding author.
E-mail address: andrew.french@ars.usda.gov (A.N. French).

0309-1708/$ - see front matter Published by Elsevier Ltd.
http://dx.doi.org/10.1016/j.advwatres.2012.07.007

covariance (EC), Bowen ratio (BR), and large aperture scintillometers (LAS), all of which are currently employed in better-known measurement networks such as FLUXNET [1,2], and the Oklahoma Mesonet (www.mesonet.org). Even for these studies, ways to acquire energy flux in more locations at lower cost would be helpful for developing better spatial models for mapping surface fluxes.

Ways to overcome logistical difficulties associated with spatially heterogeneous land surfaces have been researched for many years and include estimation of *H* fluxes in simpler and less expensive ways than with the use of, for example, EC stations. By monitoring near-surface air temperatures, *H* fluxes can be inferred by evaluating the changing statistical distributions of temperatures over time. Near-surface air temperatures in particular have what Tillman [3] described as unusual, asymmetric, non-Gaussian characteristics that can be related to *H* fluxes using Monin–Obukhov (M–O) [4] similarity theory. If the relationships can be verified, then the monitoring techniques can be implemented by installing fine wire thermocouples above vegetation canopies and measuring the temperature variations at high frequencies. Having obtained *H* values, along with R_n and *G*, enforcing energy balance allows solution for *LE* fluxes by residual.

Two currently prominent approaches that utilize air temperature monitoring are surface renewal analysis (SR), and flux variance analysis (FV). The SR approach explicitly models the shape of the air temperature traces as repeated patterns of coherent turbulent air parcels exchanging heat between the surface and the overlying air. In contrast, the FV approach, considers air temperature variability scaled by friction velocity according to M–O theory.

SR analysis is based upon the importance of coherent turbulent structures in surface energy transport (e.g. [5–10]). While air movement near the surface is both coherent and random, it is the coherent component that is the significant energy transport mechanism [11]. The coherent structures are apparent in time recordings, where air temperatures gradually drift to higher or lower temperatures at 1 Hz time scales, and then abruptly return to the temperature prior to the temperature ramp. Superimposed upon these ramps are yet higher frequency temperature variations that are randomly distributed and contribute little to energy transport [12]. Important features of SR are that all the needed information for *H* estimation is contained within the temperature trace itself (i.e., wind speed data are not used), and that it is applicable for both unstable and stable conditions [13,14].

The ramps are interpreted physically as air parcels that gradually sweep through plant canopy, but then rapidly eject from the canopy top [15]. Various interpretations of the observed patterns exist [10], and the causes for the variations are diverse, including vertical wind shear [16],canopy wave motion [17], and thermally induced eddies [18]. Which interpretation applies will affect how the patterns are subsequently related to heat fluxes. Generally, the important characteristics related to *H* fluxes are the amplitude and duration of the patterns. The pattern can be identified over an averaged time using the probabilistic approach presented by Atta [12], or by more literal identification using wavelet techniques [8,19]. SR analyses have been reported for a variety of conditions, including grass [13], rangeland [20], peach orchard [21], vineyards [22], wheat and rice [23].

An alternative way to interpret air temperature traces is with the FV approach which considers temperature variability, but without the explicit coherent structure in SR. Based on M–O similarity theory, FV combines time varying air temperature and wind speeds from sensors located close to canopy tops to produce *H* flux estimates. Based in part on earlier work by numerous investigators e.g. [24–29], Tillman [3] presented seminal research using FV under unstable to close-to neutral conditions, where asymmetric, skewed time traces of near surface temperature, as represented by its first three moments were related to the M–O turbulent stability theory. Since then many studies have investigated FV as an alternative to EC measurements with reasons including its simplicity, site insensitivity and orientation insensitivity [30–32,18,33]. The FV technique may also be extended to *LE* flux estimation, though results for research since the 1990s are conflicting and unresolved, possibly because of dis-similarities in source areas between heat and water vapor [34–36]. De Bruin and Hartogensis ([37,38]) describe implementations of FV for strongly stable and strongly advective conditions by using high frequency air temperature and wind speed data. Under nearly neutral to unstable conditions, however, the only high frequency data required are air temperatures; wind speed data can be acquired as averages over longer time periods (30–60 min).

In light of these wide-ranging studies, we wished to investigate the applicability of the SR and FV for agricultural crops grown in strongly locally advective environments. Advection is the process of horizontal transport at regional and local scales [39], and can substantially affect the estimation of surface energy flux at a site because it is not quantified using standard micrometeorological observations. At local scales advection can be highly significant, possibly leading to *LE* fluxes that exceed net radiation. Such cases can occur when advection acts across contrasting surfaces, for example from dry bare soil to irrigated croplands [40]. These conditions are common in croplands in arid and semi-arid regions, where the landscape consists of a patchwork of irrigated and dryland farms.

Our concern was the ability to estimate the surface energy fluxes when advective effects become dominant and possibly cause severe plant water stress. Thus while recognizing that advection strength ranges along a continuum, and that it can occur over a variety of land cover transitions, we only consider two conditions: strongly and weakly advective events for dry-to-wet transport. For this study, strongly advective events were those when mid-day *H* fluxes become dominantly negative, leading to *LE* fluxes exceeding net radiation. For other instances, when daytime *H* fluxes are positive, conditions were considered weakly advective. Fluxes at night time were not used in this classification.

If either SR or FV can be shown to be accurate, their use could greatly help monitor the spatially varying surface fluxes under heterogeneous conditions. In 2008, the opportunity arose to test performance of the SR and FV methods in such conditions because of the undertaking of a field experiment in the Texas High Plains. By comparing SR and FV fluxes with up to 9 EC stations distributed across an agricultural site, it became feasible to assess their relative accuracies. Although these assessments do not include horizontal flux estimates, they provide side-by-side comparisons of vertical flux estimates with respect to the best available EC observations. Thus these comparisons can reveal apparent errors and biases. Thus the purpose of this study was to compare flux estimates obtained over cropland for weakly and strongly advective conditions and to evaluate their suitability for future surface energy flux studies.

2. Methods

2.1. The BEAREX 2008 Experiment

The Bushland Evapotranspiration and Agricultural Remote Sensing Experiment in 2008 (BEAREX08), conducted from May to September 2008 at Bushland, Texas (35° 11′ N, 102°06′ W, 1170 m elevation), was an intensive, multidisciplinary research study to investigate and validate different ways to measure ET over cotton. The BEAREX08 study site was located at the Conservation & Production Research Laboratory, USDA/Agricultural Research Service, a 648 ha facility located in the semi-arid Texas High Plains.

Please cite this article in press as: French AN et al. Estimation of surface energy fluxes using surface renewal and flux variance techniques over an advective irrigated agricultural site. Adv Water Resour (2012), http://dx.doi.org/10.1016/j.advwatres.2012.07.007

Deployed were a wide range of ground-based, airborne, and spaceborne instruments measuring water fluxes and land/atmospheric properties important for ET estimation. Included were nine eddy covariance stations (EC), three Bowen ratio stations, and three scintillometer pairs distributed over the BEAREX08 site (Fig. 1). See [41] in this issue for additional details.

Three EC stations were selected for this study to represent a wide range of surface conditions: Site 1NE for irrigated cotton, Site 3NW for predominantly rainfed cotton, and Site 4G for a senescent or dormant grass plot. Site 1NE was selected because moist conditions made it responsive to strongly advective conditions, while Sites 3NW and 4G were selected for reference with drier soils. Flux data from these EC stations were used as references for estimation of vertical flux accuracies for the alternative SR and FV approaches. To establish the impact of advective fluxes on total fluxes additional observations and analyses were utilized, namely air temperature and humidity data collected from six distributed micronet stations and an assessment of horizontal flux divergence [42] across field edges. Results from these analyses (described in [43]), allowed the discrimination and verification of strongly and weakly advective conditions.

Supporting plant height data were available for the two cotton sites: 1NE and 3NW. Each EC station contained a 3-D sonic anemometer, leveled and oriented due south at a measurement height of 2.25 m above the soil, an open path H2O/CO2 gas analyzer, net radiometer, two sets each of soil heat flux plates and a fine-wire thermocouple (0.05 mm diameter) placed in the midline of the sonic anemometer. Measurement heights were 2.25 m above the ground. All EC data were recorded and stored at 20 Hz time steps, then corrected according to standard procedures. Briefly, eight main steps were followed: (1) pre-processing noise reduction and spike removal [44], (2) conversion of sonic air temperatures to actual air temperature (to provide for a continuous time series due to gaps caused by fine-wire breakage) [45], (3) 2-d coordinate rotation of wind data [46], (4) compensation for sensor displacement, (5) frequency compensation [47], (6) computation of turbulent fluxes while incorporating corrections for density [48] and for buoyancy effects [49], and (7) computation of soil heat flux [50], and (8) computation of R_n using instrument specific calibration coefficients. See [43] in this issue for further details.

2.2. Surface renewal analysis

The SR approach is based on the idea that high frequency features in near surface air temperature data contain information related to vertical H flux. These ramp-like features are distinctive by their unusual intermittent, skewed and non-Gaussian shapes [3]. They are believed to be characterized by sweeps of rapidly horizontally moving air penetrating into the canopy, followed by gradual warming (or cooling) of air adjacent to vegetation during an

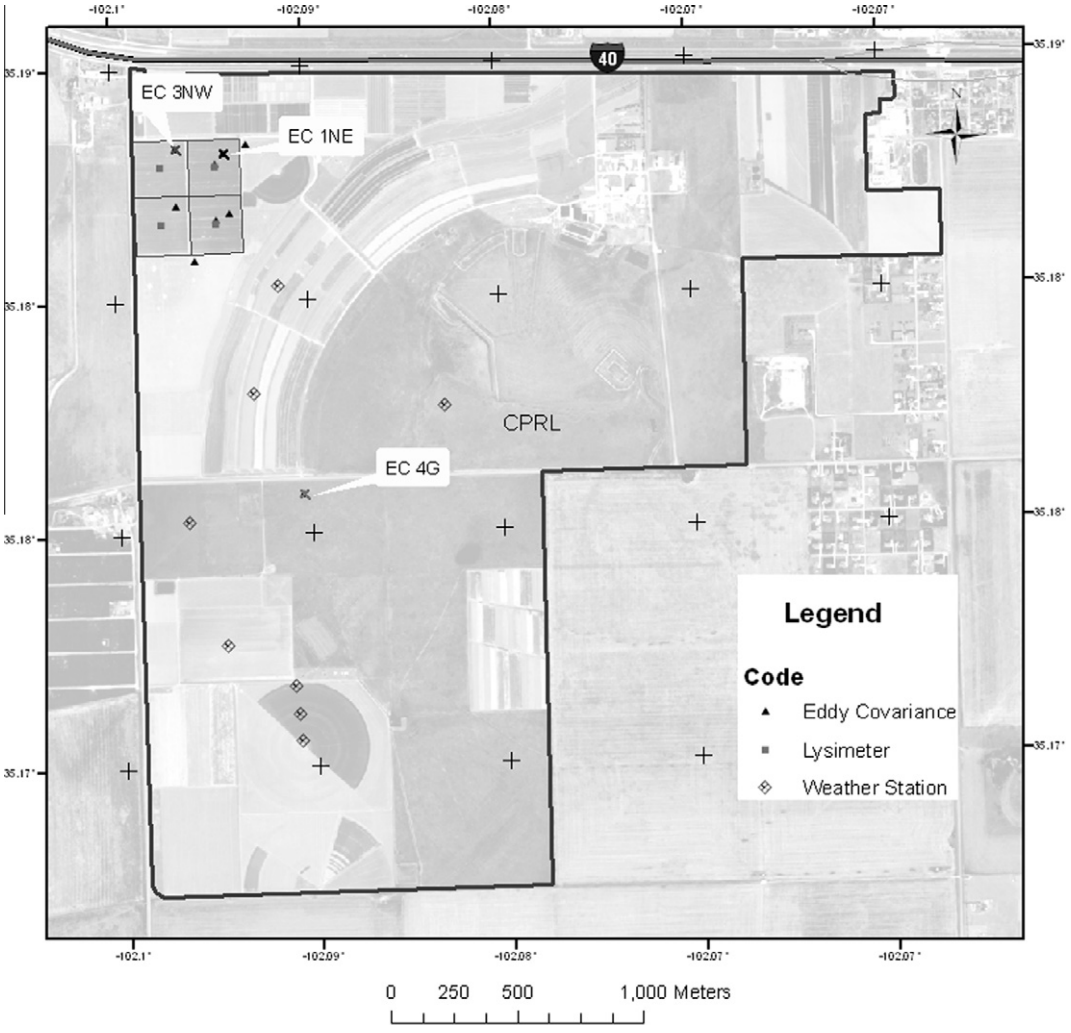

Fig. 1. BEAREX08 site location map. Two of the sites for this study, 1NE and 3NW, are located in cotton fields near the northwest corner of the USDA/ARS Conservation and Production Research Laboratory (CPRL). The third site, 4G, located in the middle left portion of the figure, was a mixture of senescent and dormant grasses.

Please cite this article in press as: French AN et al. Estimation of surface energy fluxes using surface renewal and flux variance techniques over an advective irrigated agricultural site. Adv Water Resour (2012), http://dx.doi.org/10.1016/j.advwatres.2012.07.007

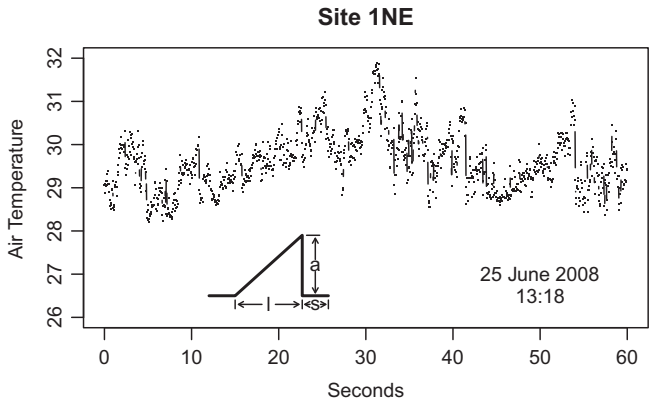

Fig. 2. Air temperature time trace at Bushland site 1NE, illustrating coherent ramp-like structures. The graphic below the time trace is scaled to match the modeled ramp dimensions. Note that high frequency variations are superimposed upon the ramp and are considered random turbulent structures.

vertically moving ejection phase. As shown in the lower part of Fig. 2, ramps can be described using three measures: ramp time duration, l (s) ramp amplitude, a (K), and a quiescent time interval s (s). Note that the graphical ramp displayed is scaled according to dimensions obtained from computational procedures applied for a 30-min time period encompassing the displayed time trace. As noted by van Atta [12], this is a simple representation of temperature changes over short times. Actual temperature traces are more complex, as in the upper part of Fig. 2, which illustrates the superposition of random high frequency temperatures changes that do not contribute to coherent turbulent energy transport.

Using a decomposition of random and coherent turbulent components, assuming time/space ergodicity, and constraining sample time lags to be much less than modeled ramp durations, Van Atta [12] formulated a probabilistic way to determine ramp duration and amplitude from second, third and fifth order structure functions, S, of the form:

$$S^n(j) = \frac{1}{m-j}\sum_{i=1+j}^{m}(T_i - T_{i-j})^n \tag{1}$$

where T_i and T_{i-j} are high-frequency temperatures measured at sequentially lagged times, j is the sample lag interval, m is the maximum sample index, i is the summation index and n is the structure function order. Eq. (1) is slightly modified form of the structure function presented in [13] and in [14], where lags are represented in time, rather than sample units. As will be discussed in 3.1, selection of lag j is important for ramp discrimination.

From analysis of the turbulent decomposition, van Atta [12] showed that the modeled ramp amplitude, is obtained by solving for the roots of the cubic equation:

$$y = a^3 + pa + q \tag{2}$$

Where the coefficient for the linear term, p, is determined from the structure functions as follows:

$$p = 10S^2(j) - \frac{S^5(j)}{S^3(j)} \tag{3}$$

And the coefficient for the offset term, q, is determined solely by the third order structure function:

$$q = 10S^3(j) \tag{4}$$

The cubic form in Eq. (2) is anti-symmetric about the y-axis with at least one real root. Potentially the solution for a is ambiguous: if $p < 0$ and the local extremes have opposite signs, then there exist three real roots. If such cases arise, likely only during transition times, the solution for a in Eq. (2) would be ambiguous. In either case roots for Eq. (2) can be found simply and quickly using Newton–Raphson iteration. In a final step, [12] shows that ramp duration in samples $(l+s)$ can be found:

$$l + s = -\frac{a^3 j}{S^3(j)} \tag{5}$$

Dividing the result of Eq. (5) by sample frequency (20 Hz for BEAREX08), returns total ramp duration time in seconds. Note that in this formulation the ramp duration sub-components are not distinguished. At this point, ways to estimate sensible of heat from temperature ramps range in complexity. A relatively simple approach is described by Snyder et al. [13], while a complex, physics-based approach is described by Castellvi et al. [51].

An idealized model [15] for sensible heat, adopted here, is:

$$H = \alpha \rho C_p \frac{a}{l+s} z \tag{6}$$

where H is sensible heat flux (W/m^2), α is a scale factor, ρ is air density (kg/m^3), C_p is the specific heat of dry air $(1013\ J\ kg^{-1}\ K^{-1})$, z is air temperature measurement height (m). Inclusion of measurement height in Eq. (6) implies that for observations within a constant flux layer that the ratio of ramp amplitude to ramp duration scales inversely with observation level.

Given different equations presented in [7,13,14], and later by Snyder et al. [15], the use of the α and height terms in Eq. (6) can be confusing. α terms are alternately height dependent and independent, while height terms can represent canopy height or measurement height. As formulated by Paw U et al. [7], α represented a height dependent calibration factor based on regressions against eddy covariance data (as part of the correction, Paw U et al. [7] also included an offset term) which was divided by two as an effort to linearly model canopy heating. Furthermore, [7] (and more recently [15]) considered z as a canopy height term, z_c. These meanings for α and z change in Snyder et al. [13,14]. Here they noted that while an $\alpha/2$ formulation worked reasonably well for trees, it did not match observations for short (<1.0–1.2 m) canopies such as for crops and grasses. By adopting a different interpretation of Eq. (6), wherein temperature fluctuations observations are representative of an air column extending to measurement height, and not to canopy height, they empirically found that setting α to 1.0 resulted in more accurate flux estimates. Accordingly, [13,14] reasoned that a value of 1.0 should be expected for observations collected well above canopy tops because of the dominance of uniform heating of air at these levels. More recently, Castellvi and Snyder [21] suggests local calibration of α against EC data.

Considering these differences, and the fact that formulations for all SR analyses require some kind of calibration, we adopted the well-documented approach described by Snyder et al. [13], meaning that α was set to 1.0 and z to measurement height.

2.3. Flux variance analysis

By comparing the standard deviation of air temperature, normalized by scaled temperature, against ζ, the stability parameter defined below, Tillman [3] showed an empirical relationship could be developed for neutral to unstable conditions:

$$H = \rho C_p u_* (\sigma_T / C_1)[C_2 - \zeta]^{-1/3} \tag{7}$$

Where the new terms are: u_* friction velocity (m/s), σ_T the standard deviation of high-frequency air temperature (K) over the averaging time, and ζ is the dimensionless stability function defined as:

$$\zeta = \frac{z - d_{om}}{L} \tag{8}$$

Please cite this article in press as: French AN et al. Estimation of surface energy fluxes using surface renewal and flux variance techniques over an advective irrigated agricultural site. Adv Water Resour (2012), http://dx.doi.org/10.1016/j.advwatres.2012.07.007

In Eq. (8), z is measurement height (m), d_{om} is the zero-displacement height (m, taken as 2/3 of plant height), and L is the Monin–Obukhov length. C_1 and C_2 in Eq. (7) are empirical constants obtained from experimental data and regression of σ_T/T_* against ζ. The C_1 parameter is a scaling factor related to the free-convection limiting condition where $\zeta \to \infty$. [4]. The C_2 parameter is an adjustment to model the other limiting condition, neutral stability, where σ_T/T_* is apparently constant. The -1/3 power on the right hand side of Eq. (7) is based on the energy spectra relationship for $-\zeta > 0.2$. As reported by Kustas et al. [31], previous studies have found that C_1 ranges between 0.95 and 1.25 [29,3,52–54]. C_2 is harder than C_1 to specify given the large uncertainties in thermal gradients under near-neutral conditions. Commonly C_2 is estimated indirectly via a third constant, C_3 , which is used when ζ approaches zero (i.e., neutral conditions). Thus when C_3 is -2.5, C_2 is 0.0549 $(= -[C_1/C_3)$, reducing Eq. (7) to:

$$H = -\rho C_p u_*(\sigma_T/C_3) \tag{9}$$

In this study, sample data were insufficient to re-specify values for C_1 , C_2 , and C_3 , thus values used by Tillman [3] were used (C_1: 0.95; C_3:-2.5).

Hence to estimate H the main requirements for the FV approach are to compute σ_T and to retrieve u_*. Note that in some instances it may be realistic to assume dominance free-convection [30], which obviates estimation of u_*. However, for this study, conditions were far from freely convecting and so this simplification could not be made. The wind speed data came from EC stations, but u_* and ζ were not derived from the sonic data, instead the equations below (Eqs. (10)–(12)) were used. This meant that relative errors in FV-derived fluxes could be ascribed inherent limitations in the C_3 parameterization. In addition, u_* was estimated in an independent way to evaluate FV performance without the benefit of the EC reference. For this we followed procedures described in [31] and in [55], who showed that u_* can be obtained from mean wind speed (u) data :

$$u_* = \frac{uk}{\left(\ln\left[\frac{(z-d_{om})}{z_{om}}\right] - \Psi_m\right)} \tag{10}$$

where z_{om} is roughness length (estimated as 1/8 of plant height), k is the van Karman constant (0.41), and Ψ_m is the integrated stability factor, determined from the equations Eqs. (11) and (12) [56–58]:

$$\Psi_m = 2\ln\left[\frac{1+x}{2}\right] + \ln\left[\frac{1+x^2}{2}\right] - 2\arctan(x) + \frac{\pi}{2} \tag{11}$$

$$x = [1 - 16\zeta]^{1/4} \tag{12}$$

Unlike the SR method, FV estimates cannot distinguish between strongly advective and weakly advective conditions. Note in Eq. (9) that H estimates are by definition non-negative for $C_3 = -2.5$. For typical weakly advective daytime conditions this constraint is not a concern. However, for the strongly advective environment at BEAREX08 this discrimination can be important. Two ways that could resolve the ambiguity are to incorporate SR methods or to compute land surface and air surface temperature differences. In the former approach, the structure skewness term (S^3) that is used in Eqs. (3) and (4) are indicators for H sign change. Since ramp amplitude changes sign in agreement with the sign of H. Another way — and the one chosen for this study because of instrument availability — distinguishes positive from negative H fluxes by monitoring the temperature gradient at half-hourly time steps. When air temperature exceeds land surface temperature, the gradient is downwards and the FV-derived H estimate is correspondingly downwards. At the three selected EC sites, surface temperatures (T_S) were estimated from upwelling ($L\uparrow$) and downwelling ($L\downarrow$) radiant flux data obtained from longwave radiometers:

$$L_S = L\uparrow - (1-\epsilon)L\downarrow \tag{13}$$

$$T_S = \sqrt[4]{L_S/\epsilon\sigma} \tag{14}$$

where ϵ is an estimate of broadband land surface emissivity (taken here to be 0.97), L_S is the land surface radiant flux W m^{-2}, σ is the Stefan–Boltzmann radiation constant (5.6705×10^{-8} W m^{-2} K^{-4}).

3. Results

Based on a review of data collected from three different EC station sites, all of which agreed within $\sim$ 17 W m^{-2} ([59]), 10 days were selected for detailed analyses. Classification of advective condition was weather-based and done as described in 1, with strongly advective conditions identified for those cases with midday H fluxes <0. Assessment by Alfieri et al. [43] in this issue shows that EC data accurately represent total fluxes even in the presence of advection: the effects due to advection were usually less than 20 W m^{-2}. Six of the selections, over the interval 25 June to 21 July, were predominantly weakly advective days, while four — 11 July, and 2, 4, and 5 August— were strongly advective. Evidence for these conditions is displayed in Table 1, which shows fluxes and winds averaged over a three-hour period between 11–14 Central Standard Time (CST). On weakly advective days the evaporative fraction (EF, i.e. $LE/[Rn - G]$) was typically 50%. On strongly advective days (gray rows) EF was close to, or exceeded 100%. With the exception of one day (5 August), mean wind speeds exceeded 3.7 m/s, characteristic of the Texas High Plains. Selection of these days was in part made to ensure that the observed fluxes were sourced from the target field locations, i.e., south of the EC positions. Variability (standard deviation) of wind direction was usually less than 20°, ensuring that the 30-min flux averages were based on representative samples.

3.1. Estimation of SR H fluxes

SR-derived H fluxes at BEAREX08 were computed from data collected at three different sites using Eqs. (1)–(6). In the SR approach, computation is straightforward, except for the selection of lag time while computing structure functions (Eq. (1)). Guidance in the literature on optimal selection of lag time is minimal. A primary constraint when using structure functions [12], is that a chosen lag should be much less than observed ramp duration times. [13] assessed SR vs. EC discrepancies and found very little sensitivity to four lag times (0.25, 0.50, 0.75, and 1.0 s) as long temperature observations were not too close, nor too far above, the canopy. However these results do not provide comprehensive evidence that lag selection has minimal impact on SR results. Considering the importance of lag time in the estimation of ramp duration, an assessment of lag selection was performed by successive analyses using a wide range: 0.1–5.0 s.

Shown in Fig. 3 are plots illustrating some of these selections and their impact upon H flux estimation accuracy. The results displayed show strong dependence upon lag time, with the best agreement returned using 1 s. This agreement held regardless of site, which meant that SR estimation accuracy was independent of surface wetness and roughness conditions. The relationship for daytime was notably stronger than for nighttime, especially since the range of H fluxes was much larger during the day. These observations suggested inconsistent ramp development at night. The best linear agreement at 1 s also closely corresponded to the ideal slope of 1, indicating that calibration of SR fluxes based on lag is a

Please cite this article in press as: French AN et al. Estimation of surface energy fluxes using surface renewal and flux variance techniques over an advective irrigated agricultural site. Adv Water Resour (2012), http://dx.doi.org/10.1016/j.advwatres.2012.07.007

Table 1
Selected strongly advective (gray) and weakly advective days for SR and FV analyses at BEAREX08.

Site 1NE							
DOY	Date	H (W m^{-2})	LE (W m^{-2})	EF (–)	U (m s^{-1})	U Direction (°)	U DirectionSD (°)
177	25 June	154	306	0.54	6.1	192	14
178	26 June	221	182	0.39	7.3	202	14
182	30 June	207	252	0.44	5.7	191	17
193	11 July	53	549	0.83	6.4	220	14
196	14 July	167	253	0.55	4.2	212	20
202	20 July	109	372	0.69	4.8	182	20
203	21 July	138	323	0.62	5.1	189	19
215	2 August	−50	639	0.97	3.7	199	25
217	4 August	−85	645	1.02	4.4	202	22
218	5 August	−12	474	0.81	1.8	159	73

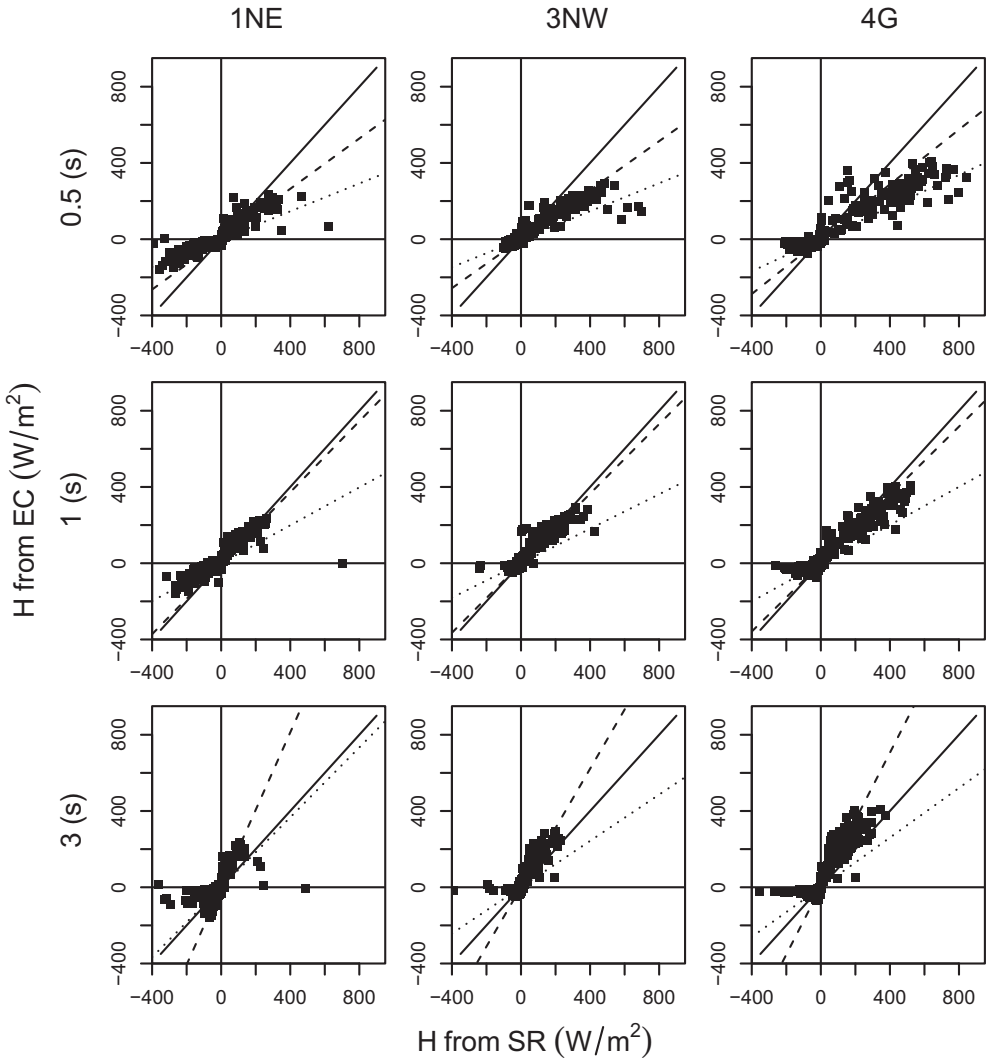

Fig. 3. Dependence of SR-based H flux estimation upon lag for all ten selected days. EC-based fluxes are plotted on the y-axis, while SR-based fluxes are plotted on the x-axis. Three lag times, displayed row-wise, were considered: 0.5, 1.0, and 3.0 s (respectively sample lags of 10, 20, and 60). The three study sites, 1NE, 3NW, and 4G, are displayed column-wise; these respectively correspond to sample lags of 10, 20, and 60. In addition to coordinate axes, there are three diagonal lines in each of the 9 plots: a solid diagonal line to indicate the 1:1 relation, a dashed line to indicate the linear regression trend for positive H fluxes, and a dotted line to indicate the regression trend for negative H fluxes. Summary statistics for the regressions are listed in Table 1.

more important consideration than the α height-dependent term, a value nominally considered close to 1.0.

The effect of lag time can be distinguished based on positive and negative H (Fig. 4) at the three observation sites. Shown are root mean square estimation errors (RMSE) and linear model slopes for SR-based H estimates relative to EC-measurements for all ten days listed in Table 1. The plots highlight an aspect not readily apparent in Fig. 3, namely that dependence of RMSE upon selected lag was non-linear, particularly for positive H. For negative H, RMSE (Fig. 4, top) generally increased with lag at all sites, but for

Please cite this article in press as: French AN et al. Estimation of surface energy fluxes using surface renewal and flux variance techniques over an advective irrigated agricultural site. Adv Water Resour (2012), http://dx.doi.org/10.1016/j.advwatres.2012.07.007

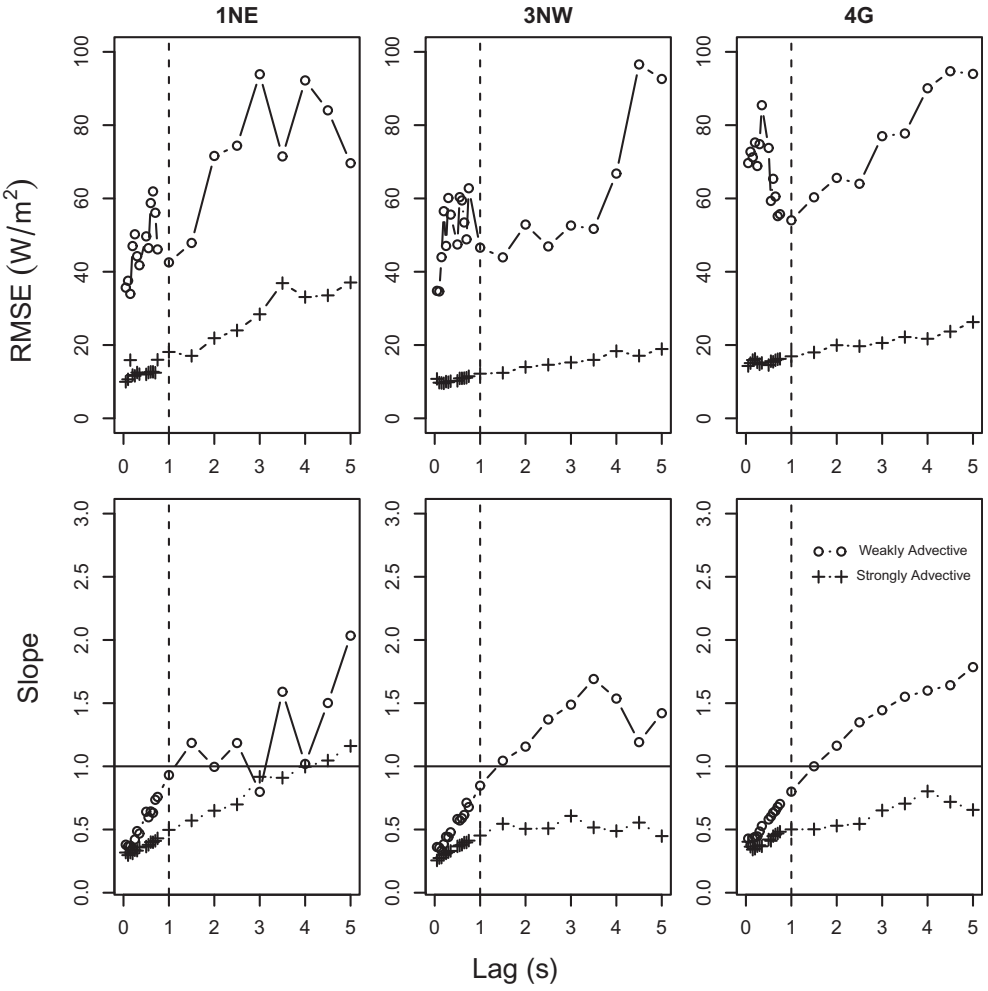

Fig. 4. SR estimation accuracies (top row) and calibration slope factors (bottom row) vs. structure function lag forthe three EC sites (displayed column-wise). Weakly advective conditions are displayed as open circles (o), and strongly advective conditions as plus signs (+). Data for strongly advective conditions were taken from 2 August; data for weakly advective conditions were taken from 25 June. For slope reference, the 1:1 relation is indicated by the solid horizontal lines. The 1.0 s lag time is indicated by vertical dashed lines.

positive H, there existed an optimal region for minimal RMSE near the 1.0 s lag time and which was on the order of 20 W m^{-2} less than for lags with shorter or long times. Existence of this RMSE minimum showed that use of either too long or too short of a lag time can greatly reduce SR estimation accuracies. When viewing dependence of the regressed slopes upon lag times (Fig. 4, bottom), the previously observed increase in slope in Fig. 3 was reflected for both negative and positive H. With the possible exception of the irrigated site 1NE, there was not a comparable optimal region where the change in the slopes of the EC to SR H relationship was minimal.

Since the choice of lag clearly had an impact upon H flux estimates, a related issue was appreciating how the lag choice affected estimation of ramp dimensions for weakly and strongly advective conditions. Using data from one time of day to illustrate the effects (13:00 CST), plots were made for ramp duration (Fig. 5, top) and ramp amplitude (Fig. 5, bottom), considering a weakly advective day, 25 June, and a strongly advective day, 2 August. The results (subsets of days used in Figs. 3 and 4) illlustrate that the impact of lag selection upon flux computations in Eq. (6) was most significant for ramp duration estimation during strongly advective conditions. As shown in Fig. 5 (top), lags at the optimal lag time of 1.0 s (corresponding to a lag of 20 samples) or greater yielded a 10 s ramp duration regardless of advection. However, choice of shorter lag times would have resulted in significantly different ramp duration estimates for strongly advective conditions. For the 2 August data set, a lag choice of 0.5 s would have yielded a ramp duration exceeding 15 s. In contrast, the results also showed that ramp amplitude estimation is stable for all but the shortest lag times, namely greater than 0.25 s (5 samples).

When considering all hours of the selected days, and not just mid-day times, the observed impact of selected lag time (1 s) did not change. Mean ramp duration values for weakly and strongly advective days differed only by a small amount, ~0.6 s (Fig. 6, top). For the same conditions, ramp amplitude differences were clearly distinguished (Fig. 6, bottom). Thus, as long as the selected lag time was not too short, lag selection critically affected ramp duration modeling, but not ramp amplitude. This suggests that even if the magnitude of the SR-based estimate of H was inaccurate, the SR approach was likely to correctly identify the direction of H flux. Henceforth, all SR estimates used 1.0 s lags.

Utilizing estimates obtained over the course of a day allowed the evaluation of the relative importance of structure function terms and how they affected the cubic equation formulations. Using Eqs. (3) and (4), the diurnal course of cubic coefficients p and q were plotted for the same weakly and strongly advective days as previously shown (Fig. 7). The roles of the coefficients in Eq. (2) are distinct. The p term controls the linear aspect of the cubic function, meaning that it determines the magnitude of the function's local minimum and maximum and hence whether of

Please cite this article in press as: French AN et al. Estimation of surface energy fluxes using surface renewal and flux variance techniques over an advective irrigated agricultural site. Adv Water Resour (2012), http://dx.doi.org/10.1016/j.advwatres.2012.07.007

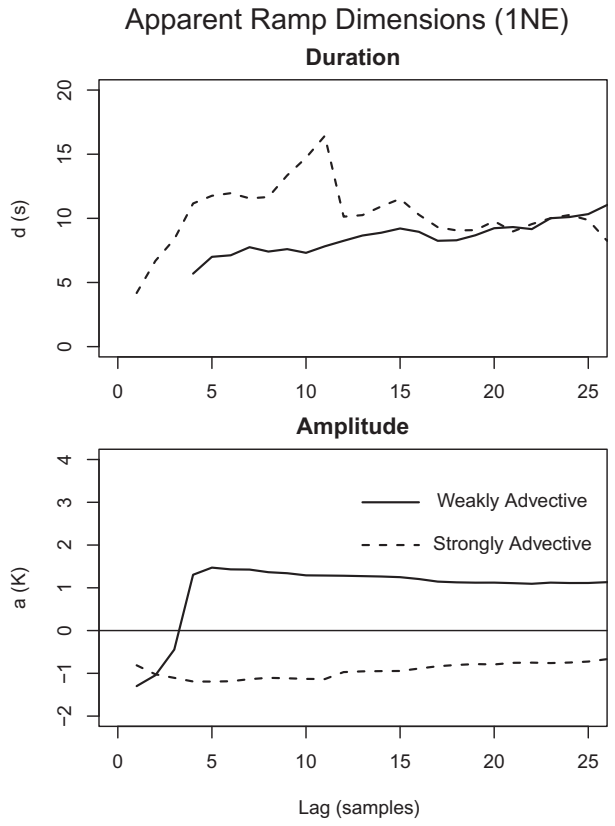

Fig. 5. Apparent ramp duration (top) and ramp amplitude (bottom) vs. sample lag. Shown are weakly advective conditions (solid) from 25 June and strongly advective conditions (dashed) from 2 August.

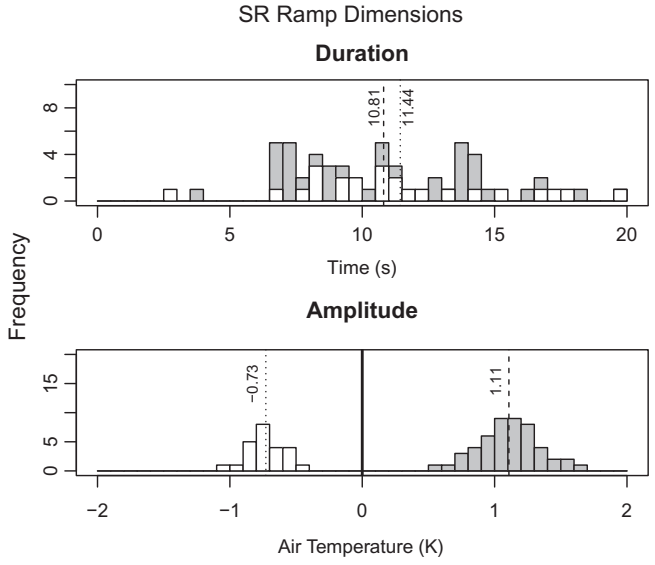

Fig. 6. Frequency distributions of SR ramp duration (top) and ramp amplitude (bottom), distinguished by mid-day weakly advective (gray) and strongly advective (white) conditions for all hours on 25 June and 2 August. Mean duration and amplitudes for weakly and strongly advective conditions are denoted by vertical dashed and dotted lines, respectively.

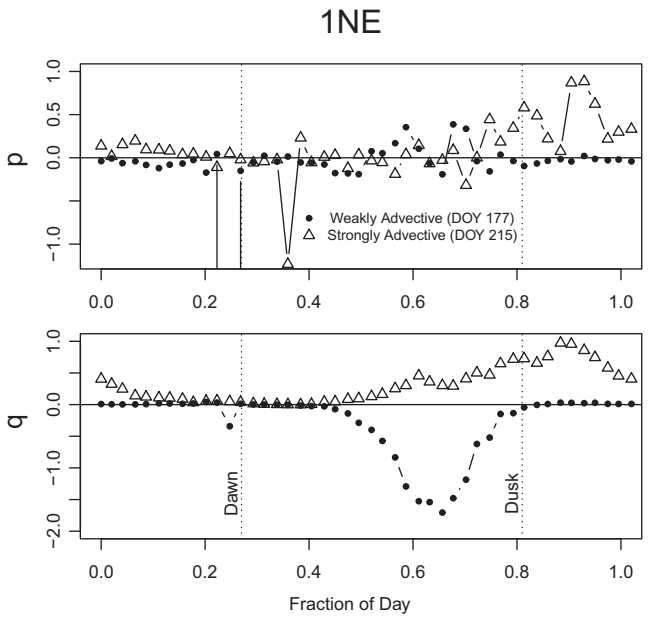

Fig. 7. Cubic function coefficients, p (top) and q (bottom), vs. time for the weakly advective day, 25 June (DOY 177, solid circles) and the strongly advective day 2 August (DOY 215, open triangles).Vertical dotted lines denote dawn and dusk.

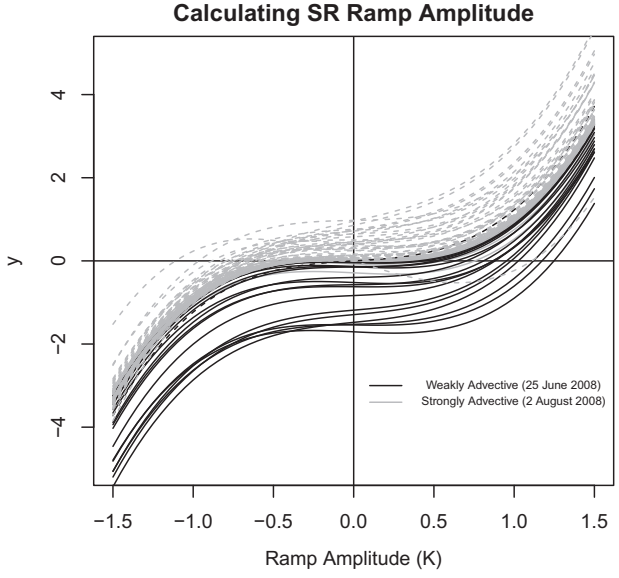

Fig. 8. Cubic functions, derived from structure functions plotted over the course of 24 hours for weakly advective day 25 June (thin black, solid) and strongly advective day 2 August (gray, dashed) at site 1NE. Thick black lines indicate functions at dawn and dusk.

not there exist multiple roots. The q term controls the cubic function vertical offset and thus is strongly influential upon root values. Except for a few outliers at dawn, and late afternoon divergence for strongly advective conditions, the p coefficient (top) generally was close to zero and thus usually unimportant. The q coefficient (bottom), on the other hand, critically controls estimation of ramp amplitude. As shown, q values showed unambiguous and smoothly varying diurnal variations. Especially for afternoon hours, the importance of the q coefficient was readily apparent, where values were negative for weakly advective conditions and positive for stronglhy advective conditions. Considering these outcomes, it was evident from Eq. (3) that 2nd and 5th order structure functions played a minor role in SR analysis, while the 3rd order function (in Eqs. 4 and 5) was crucial.

Please cite this article in press as: French AN et al. Estimation of surface energy fluxes using surface renewal and flux variance techniques over an advective irrigated agricultural site. Adv Water Resour (2012), http://dx.doi.org/10.1016/j.advwatres.2012.07.007

The geometrical representation of these roles is illustrated in Fig. 8, where the cubic functions determined by p and q terms in Fig. 7 are plotted. In the van Atta [12] approach, ramp amplitudes are determined from zero crossings. For weakly advective conditions (black lines), the crossings occurred at positive values, while for strongly advective conditions (gray lines), most zero crossings occurred at negative values. However, because the p term was close to zero, the slope of the cubic function at its inflection point was nearly horizontal. This means that if q values are also close to zero, then extraction of accurate ramp amplitudes will be difficult due to sensitivity to small variations in the third order structure function . The difficulty would be exacerbated by ambiguity from the possible existence of three roots. Fortunately for this experiment non-zero p values were uncommon and the three root problem did not arise. However, as fluxes approached zero, typically near dawn and dusk transitions, slopes at the cubic function inflection points were close to zero. This meant that SR-based estimates of ramp amplitudes were highly uncertain at these times.

3.2. Estimation of FV H fluxes

The FV approach was also implemented for all ten days and for sites 1NE, 3NW, and 4G. Estimates of H fluxes derived from the approach were obtained from standard deviations at half-hourly time steps of air temperature, computation of friction velocity using Eqs. (8), (10)–(12), and observations of mean wind speeds. Roughness length and displacement heights were derived from plant height data collected in sites 1NE, 3NW, and nominally specifying senescent grass height to be 0.3 m in site 4G. Choice of half-hourly averaging periods was made after evaluations showed hourly variability to be large during morning and early evening transition times; at these times use of hourly periods sometimes induced H estimates more than twice EC measurements. Still shorter periods could be used, although in that instance, re-analyses of EC data would need to be performed. In some cases, fine wire thermocouple data were not collected due to breakage. To fill these gaps, apparent air temperatures were obtained from the conversion of sonic air temperatures. Because the FV approach cannot distinguish between positive and negative H fluxes, longwave radiometers were used (Eqs. (13), (14)) to estimate the surface temperature, which was then compared with air temperature. Where surface temperature was less than air temperature, the FV computed H flux was assumed negative. Fig. 9 illustrates that the temperature difference approach (• symbols) closely agreed with times when $H < 0$. Shown above these are estimates based on the third-order structure function ($S3$), which also closely agree with these same times.

The results for all days, distinguished by site, are displayed in Fig. 10. The linear correlations between EC and FV positive H estimates were good for all three sites, while the negative H estimates were, as expected, poor. Because site 1NE was irrigated, advective effects were more apparent than for the other two drier sites, as evidence by the lesser number of positive H flux observations.

Results for diurnal variation of input data for the FV approach are shown in two plots (Fig. 11), emphasizing the ability of the technique is best confined to mid-day hours. At these times conditions are usually unstable and thus valid for FV theory. At other times conditions are more likely to be neutral or stable and outside the applicable range for FV. Variability for σ_T during 9:00 to 17:00 (top) was consistent and on the order of 0.2 K, while for transition times variability approached 0.5 K. Friction velocities derived from Eqs. (10)–(12) (bottom) showed a mid-day increase, corresponding to daily increases in wind speed. However, u_* values under strongly advective conditions were more than twice as variable as for weakly advective days, an outcome consistent with poor H flux estimates at those times. This larger variability was confirmed by the strong correlations ($R^2 \sim 0.82$, see Table 2) between EC-derived and FV-derived u_* values (Fig. 12, left). On the other hand, FV-derived u_* values were under-estimated, relative to EC-values, by ~16% on weakly advective days and by ~28% on strongly advective days (Fig. 12, right). Note that the relationship between u_* and H in Eq. (9) is linear, but that some non-linearity in the relationship is introduced via Eqs: (10)–(12).

Aside from temperature and windspeed observations, there is little to adjust with the FV approach. However, the 30-minute averaged EC data do allow an evaluation of the selection of C_1 and C_2 parameters needed for Eq. (7). Following the assessment done by Tillman [3], the standard deviations of air temperatures, normalized by temperature scale, were plotted against the EC-derived ζ stability parameter (Fig. 13). Using the nominal C_1 value of 0.95 constrained the relations for the straight portion of the indicated line and corresponds to the free convection condition. The nominal value for $C_3 = -2.5$ (and thus $C_2 = 0.0549$), chosen to constrain estimates under neutral conditions, corresponds to the curved portion of the solid line. Observations at BEAREX08 for near-neutral (constrained to $-\zeta > 0.01$) to slightly unstable

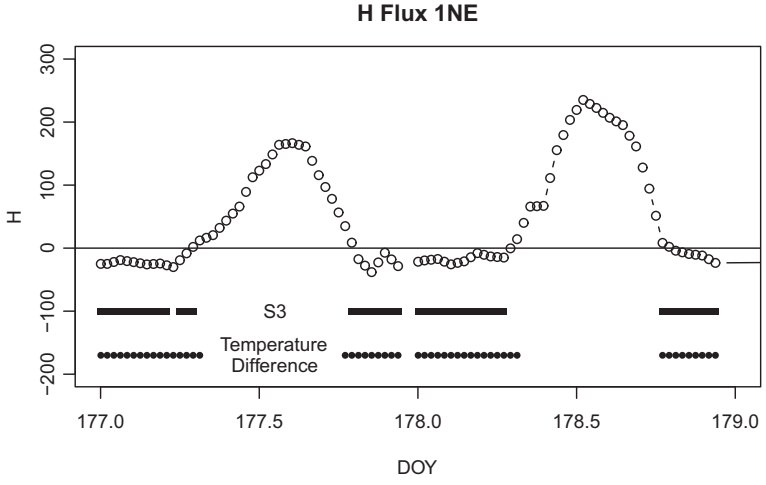

Fig. 9. Detection of negative H fluxes. The daily cycles of EC-derived H for 25–26 June 2008 (DOY 177-178), are shown with respect to two methods to locate times with negative H. One method is structure skewness (thick lines): when $S3 > 0$, temperature ramps decrease from a baseline and H is expected to be <0. Another method is the near surface air temperature/ land surface temperature difference (•symbols): when land temperature is less than air temperature, H is also expected to be <0.

Please cite this article in press as: French AN et al. Estimation of surface energy fluxes using surface renewal and flux variance techniques over an advective irrigated agricultural site. Adv Water Resour (2012), http://dx.doi.org/10.1016/j.advwatres.2012.07.007

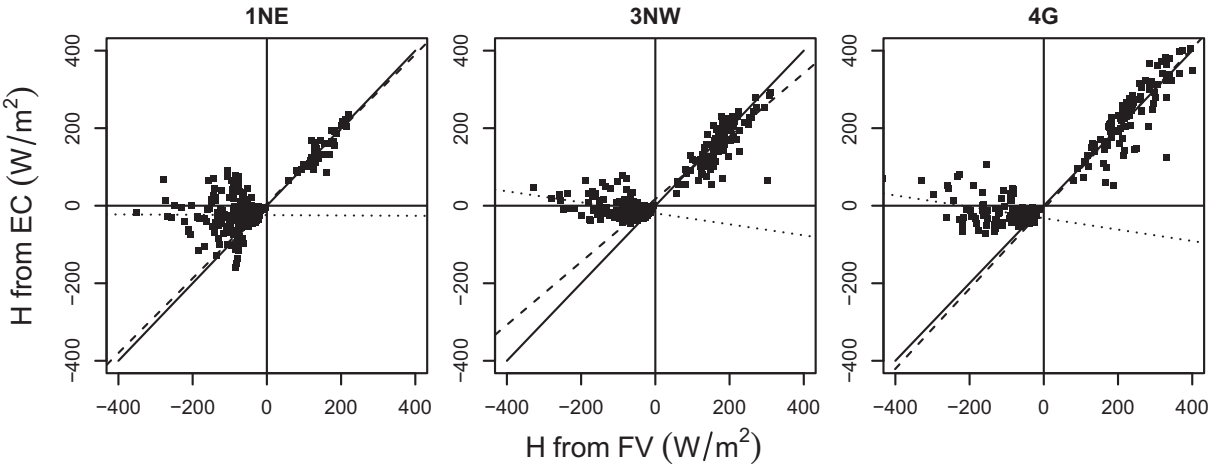

Fig. 10. FV derived *H* fluxes for all days vs. EC derived fluxes. The solid diagonal is the 1:1 line. Two sets of regression lines are shown, one dashed for positive *H*, and the other dotted for negative *H*. The regression statistics corresponding to these lines are summarized in Table 3.

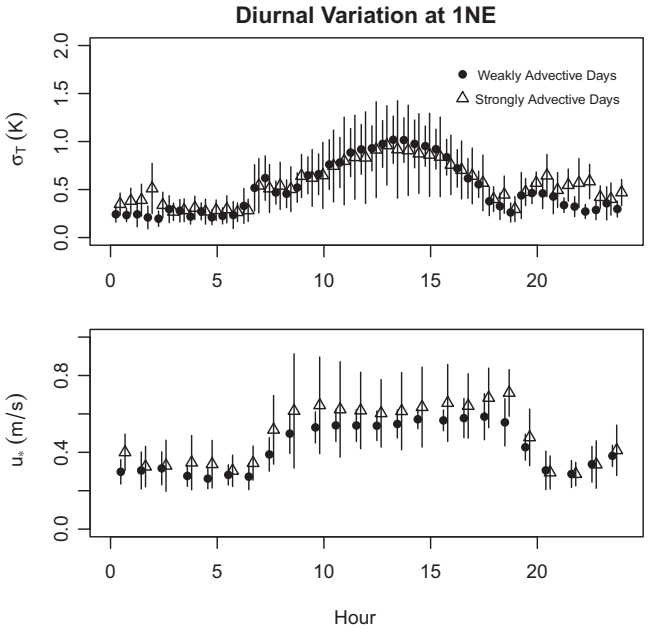

Fig. 11. Diurnal variation of parameters used for FV analysis. Displayed are half-hourly variations at site 1NE for normalized standard deviation of air temperature (top) and friction velocity (bottom). Each plot separates weakly advective days (•) from strongly advective days (△). Whiskers indicate one standard deviation. For clarity, strongly advective times are offset by 10 min.

Table 2
Effect of u_* estimation approach. The two sets of regression statistics describe the relationship between u_* estimated from windspeed data alone vs. estimates from EC data (top), and the relationship between the resulting FV *H* estimates using the different u_* values (bottom).

Advection strength	R^2	RMSE m s^{-1}	Slope (dimensionless)	Offset m s^{-1}
u_*				
Weak	0.81	0.066	0.801	0.009
Strong	0.83	0.074	0.740	0.011
FV-derived H				
Weak	0.849	28.01	0.842	16.41
Strong	0.840	38.58	0.722	38.82

conditions showed a great deal of scatter, which unfortunately means that conclusions could not be made about optimal local values for C_1 and C_2, and thus recalibration of the coefficients was not done. The scatter for neutral to slightly unstable conditions also means that FV estimates are unreliable, as previously observed by [7].

3.3. Comparison of SR and FV for weakly and strongly advective days

The overall relationship between SR and FV *H* flux estimates is summarized in Table 3. Summary statistics were analyzed by positive and negative fluxes because the FV approach was not expected to perform well in the latter instance. Generally both SR and FV methods performed well, with R^2 values on the order of 0.7 for all sites and all conditions. The FV was less sensitive to anomalous estimates for the irrigated site 1NE, yielding a lower RMSE. Similarly, regression slopes for FV estimates were close to 1 for all sites. For negative *H* instances, overall R^2 for both methods was poor, with the notable except for site 1NE, indicating that when fluxes are strongly negative the SR approach is able to detect temperature ramps.

Flux estimates for just the weakly advective days are shown in Table 4. The linear regression statistics confirm previous observations that the FV approach provides equivalent or substantially better *H* flux estimates for all three sites with respect to the SR *H* flux estimates. RMSE values from the FV approach were substantially less than SR results for the irrigated (1NE) and non-irrigated cotton (3NW) sites. RMSE values obtained from FV over the senescent/dormant grass site (4G) were slightly better than from SR. Importantly, regression slopes were close to 1.0 under FV methodology, while substantial bias appeared for the SR model. Considering the weakly advective day 25 June (DOY 177, Fig. 14), SR analysis appeared to be substantially better than FV analysis when transition times were included. Thus while FV sometimes performed better than SR during midday times, this performance was offset by less reliable estimates in early morning and late afternoon times. However these are typically when fluxes are small relative to the mid-day period. This degradation in performance was confirmed in the last portion of Table 4, where all *H* values were considered. Here SR usually excelled, with better R^2 values for all three sites and RMSE values that were approximately 50% less than obtained from FV. Exceptions occurred at site 4G, where structure function results on DOY 177 and 182 returned mid-day *H*

Please cite this article in press as: French AN et al. Estimation of surface energy fluxes using surface renewal and flux variance techniques over an advective irrigated agricultural site. Adv Water Resour (2012), http://dx.doi.org/10.1016/j.advwatres.2012.07.007

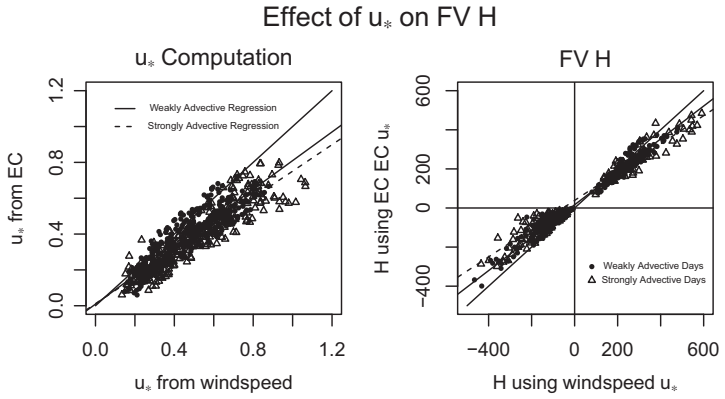

Fig. 12. Effect of u_* on FV H fluxes. u_* data estimated from EC data vs. u_* data estimated from average windspeed data and Eqs. (8), (10)–(12) are plotted on the left. Values estimated for weakly advective days are indicated by solid circles (•) and strongly advective days by triangles (△). The solid and dashed lines respectively represent linear regressions for these two sets. The thick diagonal line is the 1:1 relation. The effect of using the two different estimates of u_* are shown to the right, using the same symbology.

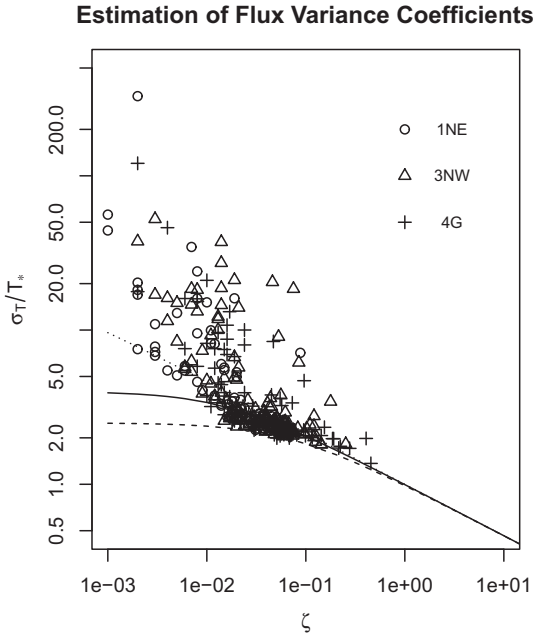

Fig. 13. Estimation of empirical FV coefficients C_1, C_2, and C_3 from normalized standard deviation of air temperature and the ζ stability parameters, both obtained from EC measurements. The solid line represents coefficients used by Tillman [3], i.e. $C_1 = 0.95$, and $C_3 = -2.5$.

estimates more than 100 W m^{-2} too great. Hence, neither SR nor FV avoided anomalous H estimates.

When considering strongly advective days (Table 5), flux results indicated no apparent advantage in either approach. This was confirmed by inspection of diurnal plots in Fig. 15. Despite the expectation that SR would outperform FV because of its inability to discriminate negative flux values, SR estimates suffered from occasional anomalous estimates. Site 1NE was the most sensitive to advective conditions due to its high moisture content; at this location SR flux estimates produced acceptable values for H with RMSE values in the range of 40–50 W m^{-2} and R^2 values ranging from 0.56 to 0.84 , indicative of a significant linear relationship with EC-derived H fluxes. The nearly equivalent RMSE values from the FV approach are indicative of the overall low H flux range, as confirmed by EC data, and not of the methods ability to accurately estimate H under advection.

4. Discussion

When assessing SR and FV results, the question arises whether or not the estimate will agree with EC data under both weakly and strongly advective conditions. Results from other studies ([7,13,14,21]) establish fairly well that both SR and FV techniques can perform well under weak advection. This study affirms that point of view: comparisons at the BEAREX08 site shows that both approaches can estimate H fluxes to ~35 W m^{-2} or better during daytime, weakly advective conditions. With the notable exception of work in California ([21]), the relative agreement of SR and FV with EC measurements under strong advection is not well known, since in these cases the development of ramp structures or the standard deviation of temperatures could be affected by fluxes sourced outside of the field of interest. At BEAREX08 during strongly advective conditions, results suggest that accuracies can be better than ~60 W m^{-2}. While there were no substantial differences between SR and FV H estimates during advection, the SR approach had an advantage because of its inherent ability to

Table 3
Statistical results comparing H flux estimates from SR and FV approaches over all ten selected days (Table 1) with respect to EC observations for all conditions at all times (0-24 CST) of day, distinguished by positive and negative fluxes.

Method	R^2			RMSE (W m^{-2})			Slope (dimensionless)			Offset (W m^{-2})		
	1NE	3NW	4G	1NE	3NW	4G	1NE	3NW	4G	1NE	3NW	4G
All days – positive H												
FV	0.74	0.66	0.33	23	34	57	0.87	0.70	0.64	−20	−9	32
SR	0.71	0.77	0.77	35	37	47	0.69	0.70	0.72	38	36	38
All days – negative H												
FV	0.01	0.66	0.12	43	22	27	0.07	−0.11	−0.12	−16	−20	−33
SR	0.59	0.07	0.04	21	12	16	0.37	0.10	0.06	−8	−14	−24

Please cite this article in press as: French AN et al. Estimation of surface energy fluxes using surface renewal and flux variance techniques over an advective irrigated agricultural site. Adv Water Resour (2012), http://dx.doi.org/10.1016/j.advwatres.2012.07.007

Table 4
H flux summary for 6 weakly advective days considering all times (0-24 CST) of day, times when *H* was positive, and mid-day times (11-14 CST). Statistics are linear regression results for comparing H from EC against H from FV.

Method	R^2			RMSE ($W\,m^{-2}$)			Slope (dimensionless)			Offset ($W\,m^{-2}$)		
	1NE	3NW	4G	1NE	3NW	4G	1NE	3NW	4G	1NE	3NW	4G
Weakly advective days – all H												
FV	0.62	0.71	0.77	50	53	63	0.41	0.45	0.56	48	46	53
SR	0.82	0.90	0.91	33	29	34	0.76	0.77	0.71	23	17	28
Weakly advective days – positive H												
FV	0.91	0.95	0.67	14	18	49	0.90	0.93	0.84	−20	−60	−12
SR	0.73	0.81	0.83	38	35	39	0.76	0.76	0.77	27	21	17
Weakly advective days – mid-day H												
FV	0.97	0.86	0.98	8	29	5	1.25	1.17	0.31	−104	−131	195
SR	0.57	0.48	0.34	34	38	42	0.52	0.44	1.00	73	92	−35

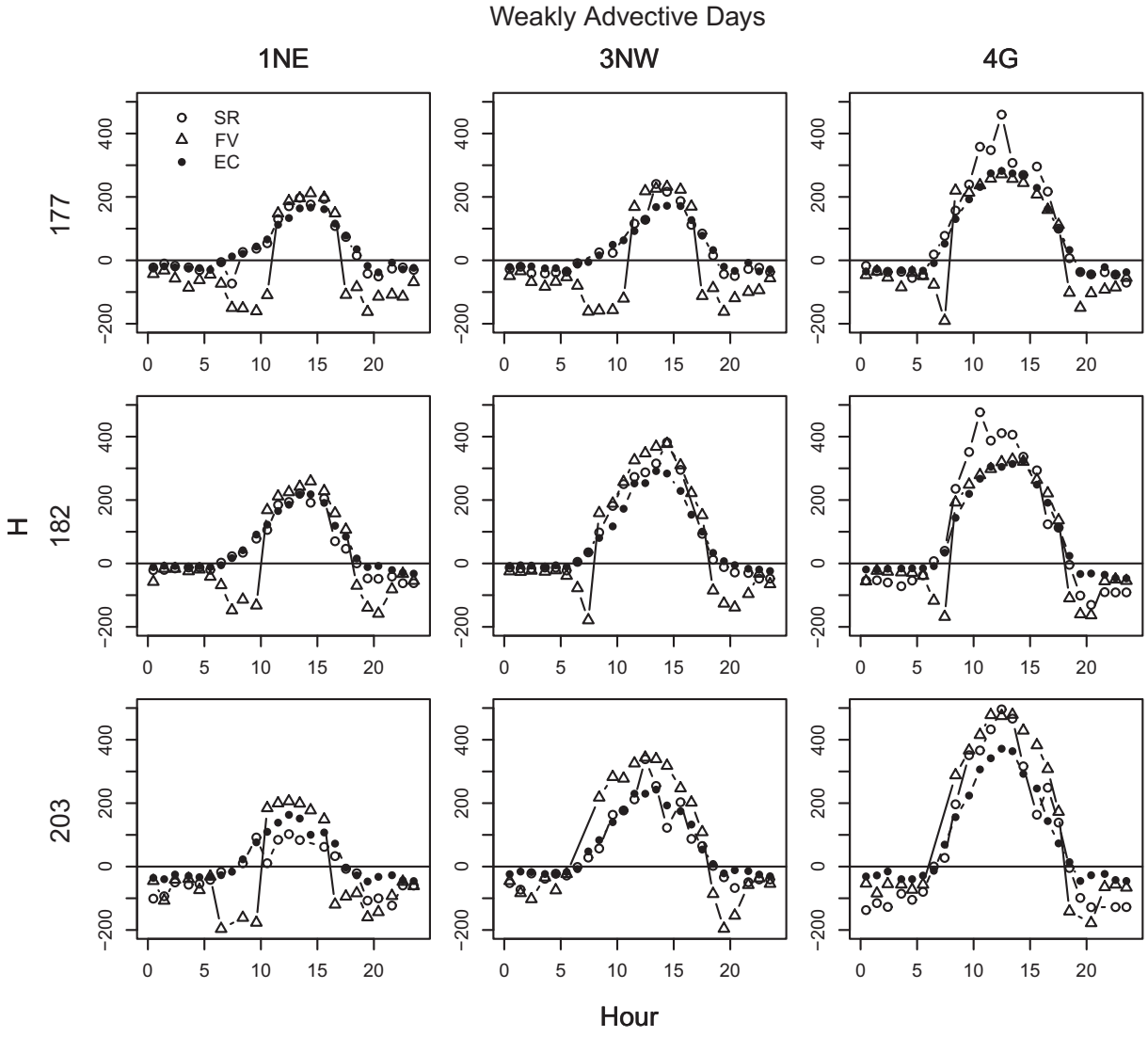

Fig. 14. Comparison of *H* fluxes derived from SR (○ symbol) and FV (△ symbol) methods with respect to EC observations (• symbol) on 25 June (177), 30 June (182), and 21 July (203) 2008, all weakly advective days. Fluxes for EC and SR data were computed at hourly time steps. FV data, computed at half-hourly time steps to reduce variability in σ_T, were averaged to hourly times.

discriminate positive and negative heat fluxes. Discrimination of *H* flux sign using land surface temperature observations reduced this obstacle for FV during strongly advective and transition times, however, utilization of shorter averaging times (30 min or less) was needed to reduce the method's sensitivity to large variations in σ_T at times other than at transition periods.

Detailed analysis of the SR approach showed that it performed well if the optimal lag time was closely matched. Although

Please cite this article in press as: French AN et al. Estimation of surface energy fluxes using surface renewal and flux variance techniques over an advective irrigated agricultural site. Adv Water Resour (2012), http://dx.doi.org/10.1016/j.advwatres.2012.07.007

Table 5
H flux summary for 3 strongly advective days for all times (0-24 CST) and for mid-day times (11-14 CST) of day. Statistics are linear regression results for comparing H from EC against H from FV.

Method	R^2			RMSE (W m^{-2})			Slope (dimensionless)			Offset (W m^{-2})		
	1NE	3NW	4G	1NE	3NW	4G	1NE	3NW	4G	1NE	3NW	4G
Strongly advective days – all H												
FV	0.04	0.74	0.76	44	45	75	0.22	0.42	0.48	−19	45	73
SR	0.56	0.78	0.84	26	41	51	0.43	0.76	0.73	−5	28	48
Strongly advective days – mid-day H												
FV	0.23	0.92	0.73	66	10	45	−0.64	0.51	0.67	−72	55	41
SR	0.00	0.54	0.10	41	35	42	0.00	0.75	0.24	−2	40	22

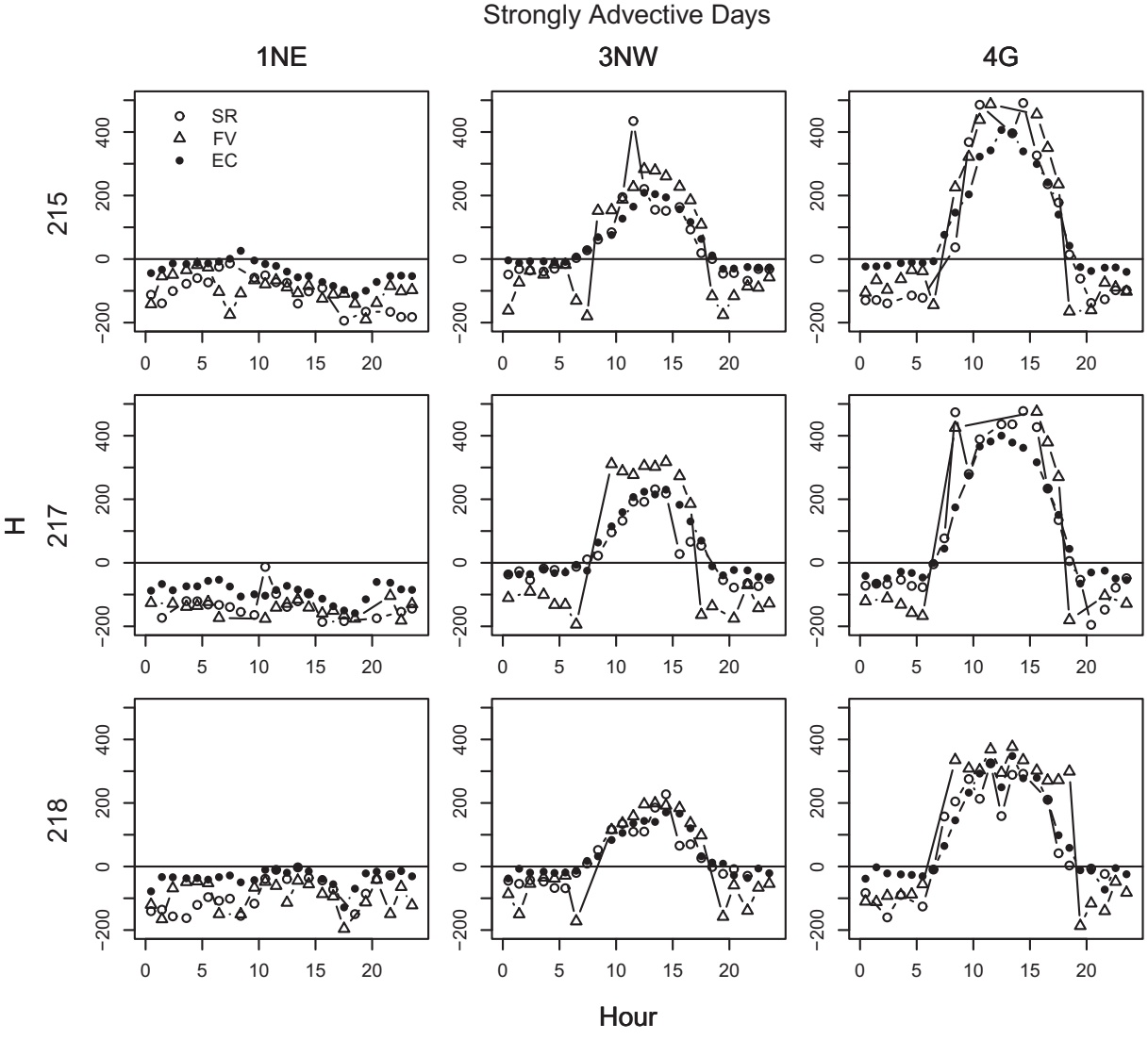

Fig. 15. Comparison of hourly *H* fluxes derived from SR ○ symbol) and FV (△ symbol) methods with respect to EC observations (• symbol) on 2 August (215), 4 August (217), and 5 August (218) 2008.

previous work [13] indicated insensitivity to lag selection (with exceptions for low and high measurement heights), this work found that selection of lags that were too short or too long significantly affected estimation accuracy of ramp duration. As noted by Chen et al. [19], misrepresentation of temperature ramps by using instantaneous terminations can lead to over-estimation of ramp durations. However, in this study, presence of such overestimates was not evaluated because optimal lags could be determined by comparison with reference EC stations. The selected lag time, 1.0 s, was consistent with lags used on other studies over crops such as cotton [15]. Absent such reference stations, time samples over more days would be needed to estimate optimal lag. Evaluation of the cubic function relationships developed by Atta [12] showed a general insensitivity to the linear term which means that instances of root finding ambiguity are likely to be uncommon. This observation implies that computation using only the third order structure function would be sufficient for SR-based *H* flux estimation.

Comparable analysis of the FV approach showed that it performed as well as, and sometimes better than, the SR approach

Please cite this article in press as: French AN et al. Estimation of surface energy fluxes using surface renewal and flux variance techniques over an advective irrigated agricultural site. Adv Water Resour (2012), http://dx.doi.org/10.1016/j.advwatres.2012.07.007

for mid-day, weakly advective conditions. RMSE H values from FV were less than SR in most cases, while R^2 values were comparable. These include conditions for which FV was developed, namely a near-neutral to unstable surface boundary layer. Considering strongly advective and stable conditions, the FV approach had similar accuracy to SR. As noted above additional longwave observations were used to resolve the flux direction of H, but results from the use the structure skewness $S3$ (illustrated in Fig. 9) show that resolution is feasible by analysis of the time-series alone. In contrast to comments by Castellví ([58]), FV at BEAREX08 required no local calibration, even though data (Fig. 11) did indicate adjustments to C_1, C_2, and C_3 could be warranted. Using nominal values established by Tillman [3], the FV method produced H flux estimates that closely matched EC data.

5. Conclusions

Analysis of air temperature data obtained in the highly advective environment during BEAREX08 showed that both FV and SR approaches can estimate H fluxes within 35–60 W m^{-2} of EC observations for midday estimates. During strongly advective conditions however, the SR approach outperformed FV during day/night transition times (when fluxes are generally small) and sometimes at nighttime: SR ramps exhibited unambiguous negative temperature ramps and diminished ramp amplitudes during dawn and dusk transition times.

The study also suggests that SR requires local calibration to optimize the chosen lag time, although the lag optimum did not have a strong dependence upon advective conditions. Overall the broader applicability of SR and its self contained approach, where wind speed data are not needed, provides the method with a logistical advantage over the FV technique.

On the other hand, the FV approach requires minimal calibration of two physically constrained empirical parameters and better agreement with EC H during peak flux periods at mid-day. FV results could be meaningful for nocturnal conditions, though theory does not extend to stable surface boundary layers. The extension would also require additional information to determine flux direction, data that could be obtained in several ways including use of thermal infrared radiometers, incorporation of structure function data (as used for SR analyses), or a 4-way net radiometer. The latter way is generally the most reliable instrument for measuring R_n [43] and is needed if LE estimates are also desired.

Suggestions have been made that SR (and by implication FV) can have lower fetch constraints than EC instruments, but both approaches face a common operational problem: how to observe high frequency air temperatures inexpensively while avoiding the practical difficulty with the use of fragile fine wire thermocouples. More robust thermocouples can be used, as was done by Kustas et al. [31], but the measurements needed to be further from the surface due to longer sensor response time, making them unsuitable for the SR technique or for areas having limited fetch. More durable two-dimensional sonic anemometers could of course be deployed, but then the simplicity and cost advantages for SR and FV are lost. If this problem can be overcome, surface energy flux estimates within strongly advective environments using EC stations can be usefully extended with either SR or FV approaches.

References

[1] Baldocchi D, Falge E, Gu L, Olson R, Hollinger D, Running S. FLUXNET: a new tool to study the temporal and spatial variability of ecosystem-scale carbon dioxide, water vapor, and energy flux densities. Bull Amer Meteorol Soc 2001;82:2415–34.
[2] Baldocchi D. Breathing of the terrestrial biosphere: lessons learned from a global network of carbon dioxide flux measurement systems. Australian J Botany 2008;56:1–26.
[3] Tillman J. The indirect determination of stability, heat and momentum fluxes in the atmospheric boundary layer from simple scalar variables during dry unstable conditions. J Appl Meteorol 1972;11:783–92.
[4] Monin A, Yaglom A. Statistical fluid mechanics. Mechanics of turbulence, 1. MIT Press; 1971.
[5] Kline S, Reynolds W, Schaub F, Runstadler P. The structure of turbulent boundary layers. J. Fluid Mech 1967;30:741–73.
[6] Raupach M, Finnigan J, Brunet Y. Coherent eddies in vegetation canopies. In: Proceedings of the Fourth Australian Conference on Heat and Mass Transfer, Christchurch, NZ, 1989, p. 75–90.
[7] Paw UK, Qiu J, Su H, Watanabe T, Brunet Y. Surface renewal analysis: a new method to obtain scalar fluxes with velocity data. Agr Forest Meteorol 1995;74:119–37.
[8] Qiu J, Paw UK, Shaw R. Pseudo-wavelet analysis of turbulence patterns in three vegetation layers. Boundary-Layer Meteorol 1995;72:177–204.
[9] Zapata N, Martinez-Cob A. Estimation of sensible and latent heat flux from natural sparse vegetation surfaces using surface renewal. J Hydrol 2001;254:215–28.
[10] Zhang Y, Liu H, Foken T, Williams Q, Mauder M, Thomas C. Coherent structures and flux contribution over an inhomogeneously irrigated cotton field. Theor Appl Climatol 2011;103:119–31.
[11] Shaw R, Paw UK, Gao W. Detection of temperature ramps and flow structures at a deciduous forest site. Agr Forest Meteorol 1989;47(2–4):123–38.
[12] Van Atta C. Effect of coherent structures on structure functions of temperature in the atmospheric boundary layer. Arch Mech 1977;29(1):161–71.
[13] Snyder R, Spano D, Paw UK. Surface renewal analysis for sensible and latent heat flux density. Boundary-Layer Meteorol 1996;77:249–66.
[14] Spano D, Snyder R, Duce P, Paw UK. Surface renewal analysis for sensible heat flux density using structure functions. Agr Forest Meteorol 1997;86:259–71.
[15] Paw UK, Snyder R, Spano D, Su HB. Surface renewal estimates of scalar. Exchange 2005.
[16] Gao W, Shaw R, Paw UK. Observation of organized structure in turbulent flow within and above a forest canopy. Boundary-Layer Meteorol 1989;47:349–77.
[17] Cava D, Giostra U, Siqueira M, Katul G. Organised motion and radiative perturbations in the nocturnal canopy sublayer above an even-aged forest. Boundary-Layer Meteorol 2004;112:129–57.
[18] Wesson K, Katul G, Lai C. Sensible heat flux estimation by flux variance and half-order time derivative methods. Water Resour Res 2001;37:2333–43.
[19] Chen W, Novak MD, Black T, Lee X. Coherent eddies and temperature structure functions for three contrasting surfaces: I. Ramp model with finite microfront time. Boundary-Layer Meteorol 1997;84:99–123.
[20] Castellví F, Snyder R, Baldocchi D. Surface energy-balance closure over rangeland grass using the eddy covariance method and surface renewal analysis. Agr Forest Meteorol 2008;148:1147–60.
[21] Castellví F, Snyder R. Sensible heat flux estimates using surface renewal analysis: a case study over a peach orchard. Agr Forest Meteorol 2009;149:1397–402.
[22] Spano D, Snyder R, Duce P, Paw UK. Estimating sensible and latent heat flux densities from grapevine canopies using surface renewal. Agr Forest Meteorol 2000;104:171–83.
[23] Zhao X, Liu Y, Tanaka H, Hiyama T. A comparison of flux variance and surface renewal methods with eddy covariance. Select Topics Appl Earth Observat Remote Sensing J IEEE 2010;3(3):345–50.
[24] Mordukhovich M, Tsvang L. Direct measurement of turbulent flows at two heights in the atmospheric ground layer. Izv Akad Sci Russ Atmos Oceanic Phys Engl Transl 1966;2:786–803.
[25] Businger J, Miyake M, Dyer A, Bradley E. On the direct determination of the turbulent heat flux near the ground. J Appl Meteorol 1967;6:1025–32.
[26] Wesely M, Thurtell G, Tanner C. Eddy correlation measurement of sensible heat flux near the earths surface. J Appl Meteorol 1970;9:45–50.
[27] McBean G. The variation of the statistics of wind, temperature and humidity fluctuations with stability. Boundary-Layer Meteorol 1971;1:438–57.
[28] Phelps G, Pond S. Spectra of the temperature and humidity fluctuations and of the fluxes of moisture and sensible heat in the marine boundary layer. J Atmosp Sci 1971;28:918–28.
[29] Wyngaard J, Coté O, Izumi Y. Local free convection, similarity, and the budgets of shear stress and heat flux. J Atmosp Sci 1971;7:1171–82.
[30] Lloyd CR, Culf A, Dolman A, Gash J. Estimates of sensible heat flux from observations of temperature fluctuations. Boundary-Layer Meteorol 1991;57:311–22.
[31] Kustas W, Blanford J, Stannard D, Daughtry C, Nichols W, Weltz M. Local energy flux estimates for unstable conditions using variance data in semiarid rangelands. Water Resour Res 1994;30(5):1351–61.
[32] Katul G, Hsieh C, Oren R, Ellsworth D, Phillips N. Latent and sensible heat flux predictions from a uniform pine forest using surface renewal and flux variance methods. Boundary-Layer Meteorol 1996;80:249–82.
[33] Choi T, Hong J, Kim J, Lee H, Asanuma J, Ishikawa H, et al. Turbulent exchange of heat, water vapor, and momentum over a Tibetan prairie by eddy covariance and flux variance measurements. J Geophys Res 2004;109:D21106.
[34] Weaver H. Temperature and humidity flux-variance relations determined by one-dimensional eddy correlation. Boundary-Layer Meteorol 1990;53:77–91.
[35] Katul G, Goltz S, Hsieh CI, Cheng Y, Mowry F, Sigmon J. Estimation of surface heat and momentum fluxes using the flux-variance method above uniform and non-uniform terrain. Boundary-Layer Meteorol 1995;74:237–60.

Please cite this article in press as: French AN et al. Estimation of surface energy fluxes using surface renewal and flux variance techniques over an advective irrigated agricultural site. Adv Water Resour (2012), http://dx.doi.org/10.1016/j.advwatres.2012.07.007

[36] Guo X, Zhang H, Cai X, Kang L, Zhu T, Leclerc M. Flux-variance method for latent heat and carbon dioxide fluxes in unstable conditions. Boundary-Layer Meteorol 2009;131:363–84.
[37] Bruin HD, Bink N, Kroon L. Flfluxes in the surface layer under advective conditions. In: Workshop on land surface evaporation measurement and parameterization. New York: Springer-Verlag; 1991. p. 157–69.
[38] Bruin HD, Hartogensis O. Variance method to determine turbulent fluxes of momentum and sensible heat in the stable atmospheric surface layer. Boundary-Layer Meteorol 2005;116:385–92.
[39] Brakke T, Verma S, Rosenberg N. Local and regional components of sensible heat advection. J Appl Meteorol 1978;17:955–63.
[40] Rider N, Philip J, Bradley E. The horizontal transport of heat and moisture – a micrometeorological study. Quarterly J Royal Meteorol Soc 1963;89:507–31.
[41] Evett S, Schwartz R, Howell TA, Baumhardt RL, Copeland K. Did weighing lysimeter ET represent surrounding field ET determined by neutron probe soil water balance for BEAREX08? Adv Water Res, 2012; this issue.
[42] Prueger J, Hipps L, Cooper D. Evaporation and the development of the local boundary layer over an irrigated surface in an arid region. Agr Forest Meteorol 1996;78:223–37.
[43] Alfieri J, Kustas W, Prueger J, Hipps L, Evett S, Basara J. On the discrepancy between eddy covariance and lysimetry-based surface flux measurements under strongly advective conditions. Adv Water Res 2012; this issue.
[44] Goring D, Nikora V. Despiking acoustic Doppler velocimeter data. J Hydraulic Eng 2002;128:117–26.
[45] Kaimal J, Gaynor J. Another look at sonic thermometry. Boundary-Layer Meteorol 1991;56:401–10.
[46] Tanner C, Thurtell G. Anemoclinometer measurements of reynolds stress and heat transport in the atmospheric surface layer. Tech. Rep.; Research and Development Technical report ECOM 66-G22-F to the U.S. Army Electronics Command, Department of Soil Science, University of Wisconsin; 1969.
[47] Massman W. A simple method for estimating frequency response corrections for eddy covariance systems. Agr Forest Meteorol 2000;104:185–98.
[48] Webb E, Pearman G, Leuning R. Correction of flux measurements for density effects due to heat and water vapour transfer. Q J Roy Meteor Soc 1980;106:85–100.
[49] Foken T. The energy balance closure problem: an overview. Ecol Appl 2008;18:1351–67.
[50] Oke T. Boundary layer climates. New York: Routledge; 1987.
[51] Castellví F, Snyder R, Baldocchi D, Martinez-Cob A. A comparison of new and existing equations for estimating sensible heat flux using surface renewal and similarity concepts. Water Resour Res 2006;42.
[52] Hicks B, An analysis of Wangara micrometeorology: surface stress, sensible heat, evaporation, and dewfall. Tech. Rep.; NOAA Tech. Memo. ERL ARL-104, NOAA/Air Resources Laboratories, Silver Spring, MD, 1981.
[53] Wesely M. Use of variance techniques to measure dry air-surface exchange rates. Boundary-Layer Meteorol 1988;44:13–31.
[54] Kader B, Yaglom A. Mean fields and fluctuation moments in unstable stratified turbulent boundary layers. J Fluid Mech 1990;212:637–62.
[55] Brutsaert W. Evaporation into the atmosphere: theory, history, and applications. Dordrecht, Holland: Reide; 1982.
[56] Dyer A. A review of the flux-profile relationships. Boundary-Layer Meteorol 1974;7:363–72.
[57] Högström U. Non-dimensional wind and temperature profiles in the atmospheric surface layer: a re-evaluation. Boundary-Layer Meteorol 1988;42:55–78.
[58] Castellví F. Combining surface renewal analysis and similarity theory: a new approach for estimating sensible heat flux. Water Resour Res 2004;40:W052011–W0520120.
[59] Alfieri J, Kustas W, Prueger J, Hipps L, Chavez J, French A, et al. Intercomparison of nine micrometeorological stations during the BEAREX08 field campaign. J Atmos Oceanic Tech 2011;11:1390–406.

Please cite this article in press as: French AN et al. Estimation of surface energy fluxes using surface renewal and flux variance techniques over an advective irrigated agricultural site. Adv Water Resour (2012), http://dx.doi.org/10.1016/j.advwatres.2012.07.007